

Article

# A Mathematical Model to Predict Diagnostic Periods for Secondary Distant Metastases in Patients with ER/PR/HER2/Ki-67 Subtypes of Breast Cancer

Ella Ya. Tyuryumina <sup>1,\*</sup> , Alexey A. Neznanov <sup>1</sup>  and Jacob L. Turumin <sup>2</sup>

<sup>1</sup> International Laboratory for Intelligent Systems and Structural Analysis, Faculty of Computer Science, National Research University Higher School of Economics, 109028 Moscow, Russia; aneznanov@hse.ru

<sup>2</sup> Medical Center “For all Family”, 664047 Irkutsk, Russia; yatyuryumin@gmail.com

\* Correspondence: etyuryumina@hse.ru

Received: 19 July 2020; Accepted: 17 August 2020; Published: 19 August 2020



**Abstract:** Previously, a consolidated mathematical model of primary tumor (PT) growth and secondary distant metastasis (sdMTS) growth in breast cancer (BC) (CoMPaS) was presented. The aim was to detect the diagnostic periods for visible sdMTS via CoMPaS in patients with different subtypes ER/PR/HER2/Ki-67 (Estrogen Receptor/Progesterone Receptor/Human Epidermal growth factor Receptor 2/Ki-67 marker) of breast cancer. CoMPaS is based on an exponential growth model and complementing formulas, and the model corresponds to the tumor-node-metastasis (TNM) staging system and BC subtypes (ER/PR/HER2/Ki-67). The CoMPaS model reflects (1) the subtypes of BC, such as ER/PR/HER2/Ki-67, and (2) the growth processes of the PT and sdMTSs in BC patients without or with lymph node metastases (MTSs) in accordance with the eighth edition American Joint Committee on Cancer prognostic staging system for breast cancer. CoMPaS correctly describes the growth of the PT in the ER/PR/HER2/Ki-67 subtypes of BC patients and helps to calculate the different diagnostic periods, depending on the tumor volume doubling time of sdMTS, when sdMTSs might appear. CoMPaS and the corresponding software tool can help (1) to start the early treatment of small sdMTSs in BC patients with different tumor subtypes (ER/PR/HER2/Ki-67), and (2) to consider the patient almost healthy if sdMTSs do not appear during the different diagnostic periods.

**Keywords:** breast cancer; secondary distant metastases; survival; tumor volume doubling time; ER/PR/HER2/Ki-67; mathematical model

## 1. Introduction

After the primary tumor (PT) of breast cancer (BC) is diagnosed, multimodal treatment occurs, including surgery (lumpectomy, unilateral or bilateral mastectomy), radiotherapy, and chemotherapy [1]. However, different parameters, such as the size of the PT, the number of affected lymph nodes, and the growth rate of metastases (MTSs), influence the appearance of secondary distant metastases (sdMTSs) in different organs [2–15]. Moreover, these different parameters determine the period from resection of the PT to the first clinical manifestation of sdMTSs (MTS-free survival time or non-visible period) [8,9,13,16–21]. Although the interval of time from the date of diagnosis (using the tumor-node-metastasis (TNM) staging system) to the date of the patient’s death is referred to as survival (lifetime), it is commonly defined as a rate per hundred living patients for a certain period after the diagnosis [1,10,11,14,15]. Hence, survival includes the non-visible growth period (MTS-free period) and the visible growth period of sdMTSs, diagnostics, treatment, and patient death [21]. PTs of breast cancer grow at different rates: rapid, intermediate, and slow [2–4,6,7]. The growth rate of sdMTSs depends on the growth rate of the PT [2–4,6,7]. The growth rate of

PTs in BC may depend on different subtypes of ER/PR/HER2/Ki-67 (Estrogen Receptor/Progesterone Receptor/Human epidermal growth factor Receptor 2/Ki-67 marker) expression in BC [22–26].

The current guidelines on BC follow-up recommend regular visits. The European Society of Medical Oncology (ESMO) recommends follow-up visits every 3–4 months after resection of the PT for the first two years [27]. The American Cancer Society/American Society of Clinical Oncology (ASCO) recommends follow-up visits every 3–6 months after resection of the PT for the first three years, every 6–12 months for the next two years, and every 12 months after the first five years [28].

The National Comprehensive Cancer Network (NCCN) recommends follow-up visits every 4–6 months after resection of the PT for the first five years and every 12 months after the first five years [29]. The Associazione Italiana di Oncologia Medica (AIOM) recommends follow-up visits every 3–6 months after resection of the PT for the first five years and every 12 months after the first five years [29].

The guidelines recommend performing annual examinations, including bilateral (in the case of organ-preserving surgery) or contralateral mammography, a computed tomography of the thoracic organs, and an ultrasound examination of the abdominal organs [1,27–32].

All BC patients receive comprehensive PT treatment. The duration of the sdMTS-free period depends equally on both the metastatic tumor rate and the duration of the preclinical non-visible growth period of BC (doubling time) [7,21,33–42].

Case studies from the BC field show that mathematical models can provide tangible advantages [7,10–12,14–21,33–42]. For instance, a consolidated mathematical model of PT growth and sdMTS growth in BC (CoMPaS) allows the calculation of the number of doublings and the tumor volume doubling time (TVDT) (days) for the different growth periods throughout the whole BC process [21].

The current guidelines for multimodal examinations are generalized to all patients [43]. Consequently, there is a lack of personalized recommendations for multimodal examinations to detect sdMTSs in patients with BC with regard to the stage and/or the growth rate of the PT. All patients with BC worry about the appearance of sdMTSs after resection of the PT. Thus, the most important question is whether sdMTSs will appear.

If sdMTSs do appear, when will the sdMTSs first materialize? The available clinical studies provide no information about the period of manifestation of sdMTSs after PT resection in each patient as a function of the size of the PT and the stage of the BC. The problem becomes very complex because the patients must obtain a personalized approach to build a schedule of multimodal examinations to detect sdMTSs at the early stage and to start early treatment, which can increase the patient's lifetime. Currently, the possibility of calculating the earliest diagnostic period of sdMTSs in patients with BC, taking into account the stage and/or the growth rate of the PT, was not proposed in any mathematical model in the available studies.

Moreover, if sdMTSs do not appear, when will the patient be considered healthy? Currently, there is no answer to this question.

The purpose of this study was to answer these questions using the model CoMPaS, considering the TNM stage and ER/PR/HER2/Ki-67 subtypes. Therefore, the aim of the research was to detect the personalized diagnostic periods for visible sdMTS via CoMPaS in patients with different subtypes (ER/PR/HER2/Ki-67) of breast cancer. The personalized diagnostic periods for multimodal examinations during the MTS-free period were calculated in BC patients depending on the TVDT of PT and TVDT of sdMTSs.

## 2. Results

### 2.1. Consolidated Mathematical Growth Model of Primary Tumor and Secondary Distant Metastases (CoMPaS) in Patients with ER/PR/HER2/Ki-67 Subtypes and Stage I/II/III of Breast Cancer with or without Metastases in the Lymph Nodes

The CoMPaS model helps to determine the causes of BC appearance, which can lead to the development of prevention methods and a deeper understanding of the BC process (Figure 1; Table 1) [21].

sdMTSs are formed from the metastatic cells of the metastasizing PT. The diameter of the metastasizing PT may vary in size from 1 mm up to the diameter of the PT at the time of resection (non-visible MTS-I period) (Figure 1).

**Table 1.** Diagnostic periods for sdMTSs in patients with ER/PR/HER2/Ki-67 (Estrogen Receptor/Progesterone Receptor/Human Epidermal growth factor Receptor 2/Ki-67 marker) subtypes of BC for stage T1cN0-3M0. TVDT—tumor volume doubling time.

	T1c (mm) 10 < d ≤ 20	T1c (mm) 10 < d ≤ 20	T1c (mm) 10 < d ≤ 20	T1c (mm) 10 < d ≤ 20	T1c (mm) 10 < d ≤ 20
d <sub>PT</sub> at surgery (mm)	15.1	15.1	15.1	15.1	15.1
PT <sub>log(V)</sub>	31.7	31.7	31.7	31.7	31.7
TVDT <sub>PT</sub> (days)	80–110–135	136–150–165	166–180–195	196–210–230	231–250–270
TVDT <sub>PT</sub> (days) mean	110	150	180	210	250
	V subtype	IV subtype	III subtype	II subtype	I subtype
Good prognosis					I subtype
Very slow growth rate					HR(+)/Her2(–)
TVDT <sub>MTS</sub> (days)				230(+)	231–270
Mean TVDT <sub>MTS</sub> (days)				230(+)	116–135
d <sub>MTS</sub> (mm)				9.0	9.0
Non-visible MTS(1-X)-I				7.41–14.80	7.43–8.69
Non-visible MTS(1-X)-II				11.19–18.58	11.23–13.13
Visible MTS(1-X) (years)				6.66–14.05	6.68–7.81
Survival MTS(1-X) (years)				17.84–25.23	17.91–20.93
Period of MTS(1-X) diagnosis				7.40	1.95
Screening time				12 mo	12 mo
Intermediate prognosis				II subtype	
Slow growth rate				HR(+)/Her2(+)	
TVDT <sub>MTS</sub> (days)			195(+)	196–230	196–230
Mean TVDT <sub>MTS</sub> (days)			195(+)	98–115	98–115
d <sub>MTS</sub> (mm)			9.0	9.0	9.0
Non-visible MTS(1-X)-I			6.28–12.55	6.31–7.40	6.31–7.40
Non-visible MTS(1-X)-II			9.49–15.76	9.53–11.18	9.53–11.18
Visible MTS(1-X) (years)			5.65–11.91	5.67–6.65	5.67–6.65
Survival MTS(1-X) (years)			15.13–21.39	15.20–17.83	15.20–17.83
Period of MTS(1-X) diagnosis			6.27	1.70	1.70
Screening time			8 mo	8 mo	8 mo
Intermediate prognosis				III subtype	
Intermediate growth rate				HR(+)/HER2(–)	
TVDT <sub>MTS</sub> (days)		165(+)	166–195	166–195	166–195
Mean TVDT <sub>MTS</sub> (days)		165(+)	83–97	83–97	83–97
d <sub>MTS</sub> (mm)		9.0	9.0	9.0	9.0
Non-visible MTS(1-X)-I		5.32–10.62	5.34–6.27	5.34–6.27	5.34–6.27
Non-visible MTS(1-X)-II		8.03–13.33	8.07–9.48	8.07–9.48	8.07–9.48
Visible MTS(1-X) (years)		4.78–10.08	4.80–5.64	4.80–5.64	4.80–5.64
Survival MTS(1-X) (years)		12.80–18.10	12.87–15.12	12.87–15.12	12.87–15.12
Period of MTS(1-X) diagnosis		5.31	1.46	1.46	1.46
Screening time		6 mo	6 mo	6 mo	6 mo
Intermediate prognosis				IV subtype	
Intermediate growth rate				HR(–)/HER2(+)	
TVDT <sub>MTS</sub> (days)	135(+)	136–165	136–165	136–165	136–165
Mean TVDT <sub>MTS</sub> (days)	135(+)	68–82	68–82	68–82	68–82
d <sub>MTS</sub> (mm)	9.0	9.0	9.0	9.0	9.0
Non-visible MTS(1-X)-I	4.35–8.69	4.38–5.31	4.38–5.31	4.38–5.31	4.38–5.31
Non-visible MTS(1-X)-II	6.57–10.91	6.61–8.02	6.61–8.02	6.61–8.02	6.61–8.02

Table 1. Cont.

	T1c (mm) 10 < d ≤ 20	T1c (mm) 10 < d ≤ 20	T1c (mm) 10 < d ≤ 20	T1c (mm) 10 < d ≤ 20	T1c (mm) 10 < d ≤ 20
Visible MTS(1-X) (years)	3.91–8.25	3.93–4.77	3.93–4.77	3.93–4.77	3.93–4.77
Survival MTS(1-X) (years)	10.48–14.81	10.54–12.79	10.54–12.79	10.54–12.79	10.54–12.79
Period of MTS(1-X) diagnosis	4.34	1.46	1.46	1.46	1.46
Screening time	5 mo	5 mo	5 mo	5 mo	5 mo
Poor prognosis	<b>V subtype</b>				
Rapid growth rate	<b>HR(-)/HER2(-)</b>				
TVDT <sub>MTS</sub> (days)	10–135	10–135	10–135	10–135	10–135
Mean TVDT <sub>MTS</sub> (days)	40–67	40–67	40–67	40–67	40–67
d <sub>MTS</sub> (mm)	9.0	9.0	9.0	9.0	9.0
Non-visible MTS(1-X)-I	0.55–4.34	0.55–4.34	0.55–4.34	0.55–4.34	0.55–4.34
Non-visible MTS(1-X)-II	0.26–6.56	0.26–6.56	0.26–6.56	0.26–6.56	0.26–6.56
Visible MTS(1-X) (years)	0.29–3.90	0.29–3.90	0.29–3.90	0.29–3.90	0.29–3.90
Survival MTS(1-X) (years)	0.55–10.47	0.55–10.47	0.55–10.47	0.55–10.47	0.55–10.47
Period of MTS(1-X) diagnosis	6.30	6.30	6.30	6.30	6.30
Screening time	3 mo	3 mo	3 mo	3 mo <td 3 mo	
Total period MTS(1-X) diagnosis	10.64	13.07	15.49	18.32	12.87

$d_{PT}$  at surgery (mm)—the mean size (mm) of the PT at surgery (resection of the PT) for each stage (T1, T2, T3), obtained from Table 1 of [15];  $PT_{log(V)}$ —the number of doublings of the PT at surgery (resection of the PT) [20,21,44–56];  $TVDT_{PT}$ —the mean tumor volume doubling time of the PT (days) at surgery (resection of the PT) [20,21,44–56];  $TVDT_{MTS}$ —the mean tumor volume doubling time of the sdMTS (days) [20,21,57–68];  $d_{MTS}$ —the mean size (mm) of the sdMTS at the diagnosis period; *Non-visible MTS(1-X)-I (years)*, *Non-visible MTS(1-X)-II (years)*, *Visible MTS(1-X) (years)* and *Period of MTS(1-X) diagnosis*—see Figure 1. *Survival MTS(1-X) (years)*—the survival (lifetime) can be calculated as the period between the date of diagnosis (using the tumor-node-metastasis (TNM) staging system) and the date of patient death. The survival of BC patients includes both the non-visible and visible growth periods of the sdMTS (the first, intermediate, or last sdMTS from the PT); *Total period of MTS(1-X) diagnosis (years)*—sum of the periods of the MTS(1-X) diagnosis (periods of rapid growth rate, intermediate growth rate, and slow and very slow growth rates). *I subtype*—Luminal A, HR(+)/Her2(-), Ki-67 < 14% for HR-positive (ER+/PR+ or ER+/PR- or ER-/PR+) tumors [22–26,69–72]; *II subtype*—Luminal B, HR(+)/Her2(+), Ki-67 ≥ 14% for HR-positive (ER+/PR+ or ER+/PR- or ER-/PR+) and Her2-positive tumors [22–26,69–72]; *III subtype*—Luminal B, HR(+)/Her2(-), Ki-67 ≥ 14% for HR-positive (ER+/PR+ or ER+/PR- or ER-/PR+) tumors [22–26,69–72]; *IV subtype*—HER2-positive, HR(-)/Her2(+), Ki-67 ≥ 14% [22–26,69–72]; *V subtype*—Triple Negative, HR(-)/Her2(-), Ki-67 ≥ 14% [22–26,69–72].

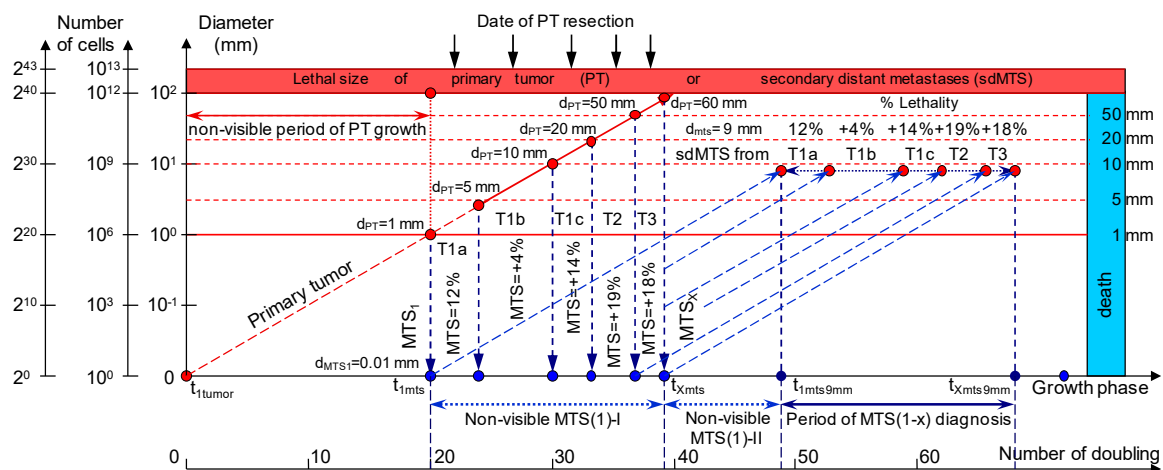


**Figure 1.** The mathematical model used to predict the earliest diagnostic period of the secondary distant metastasis (sdMTS) in patients with breast cancer (BC). T1a = 1 mm < d ≤ 5 mm; T1b = 5 mm < d ≤ 10 mm; T1c = 10 mm < d ≤ 20 mm; T2 = 20 mm < d ≤ 50 mm; T3 = d > 50 mm [14]. *Non-visible MTS(1-X)-I (years)*—the non-visible growth period of the sdMTS (the first non-visible sdMTS from the primary tumor (PT)) can be calculated as the period from the appearance of the first metastatic cell of the sdMTS (d = 10 μm) to the detection of the non-visible sdMTS (before the date of PT surgery); *Non-visible MTS(1-X)-II (years)*—the non-visible growth period of sdMTS (the first non-visible sdMTS from the PT) can be calculated as the period from the diagnosis (after date of PT surgery) to the diagnosis of the visible size (d = 9 mm) of at least one sdMTS; *Visible MTS(1-X) (years)*—the visible growth period of sdMTS(1) (the first visible sdMTS from the PT) can be calculated as the period from the diagnosis of the

visible size ( $d = 9$  mm) to when it reaches the lethal size (death); *Visible MTS(X)* (years)—the visible growth period of sdMTS(X) (the last visible sdMTS from the PT) can be calculated as the period from the diagnosis of the visible size ( $d = 9$  mm) to when it reaches the lethal size (death); *Period of MTS(1-X) diagnosis*—the period of the diagnosis of the visible size ( $d = 9$  mm) of the sdMTS from the first visible sdMTS (1) to the last visible sdMTS (X).

2.1.1. T1cN0-3M0. The Whole Natural History of the PT (Triple-Negative, HR(-)/HER2(-), Ki-67  $\geq 14$ ) and sdMTS

If the diameter of the PT at its resection,  $d_{PT}$ , was 15.1 mm (Figure 2; Table 1), and the  $TVDT_{PT}$  was 10–135 days (a rapid growth rate of PT in patients with HR(-)/HER2(-) (triple-negative) tumors), then the diameter of the sdMTS at PT resection,  $d_{MTS}$ , could be 0.01–1.00 mm.

For patients in the rapid growth rate group,  $TVDT_{MTS}$  was equal to 10–135 days. The non-visible growth period of sdMTS(1-X)-I was 0.55–4.34 years (Figure 2; Table 1). The non-visible growth period of sdMTS(1-X)-II was 0.26–6.56 years. The visible growth period of sdMTS(1-X) was 0.29–3.90 years. The survival of patients with BC was 0.55–10.47 years.

In summary, in this period of rapid growth rate of sdMTS, patients with T1cN0-3M0 BC must undergo multimodal examination every three months 0.26 years after resection of the PT for 6.30 years.

The total period of MTS(1-X) diagnosis may be 10.64 years (Figure 2; Table 1). BC patients with  $d_{PT} = 15.1$  mm and  $TVDT_{PT} = 10$ –135 days (T1aN0-3M0) may be considered healthy only after 10.64 years if sdMTSs were not diagnosed in this period.

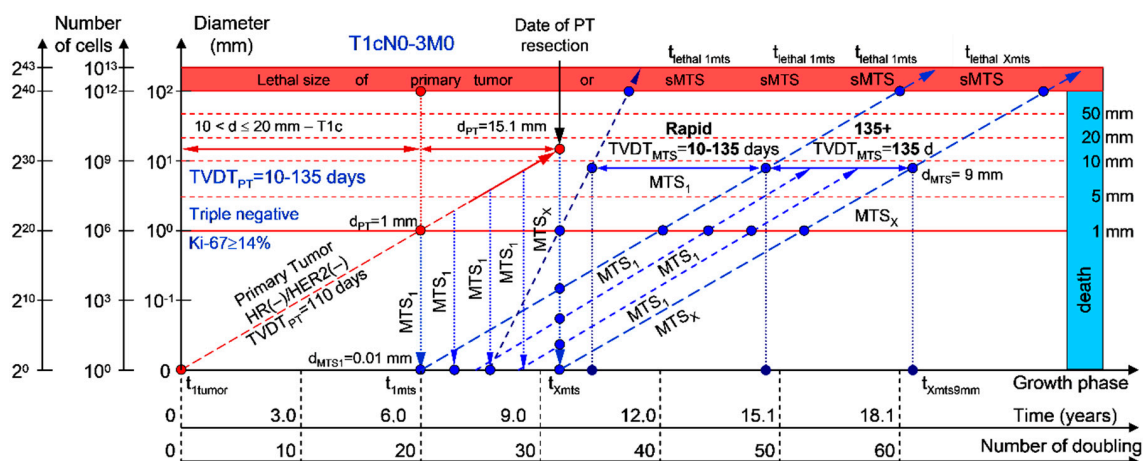


**Figure 2.** T1cN0-3M0. The whole natural history of the PT (triple-negative, HR(-)/HER2(-), Ki-67  $\geq 14$ ) and sdMTS. Parameter T1c:  $10 \text{ mm} < d \leq 20 \text{ mm}$ . Diameter of PT =  $d_{PT} = 15.1$  mm,  $TVDT_{PT} = 10$ –135 days. Rapid growth rate of secondary distant MTS =  $TVDT_{MTS} = 10$ –135 days. Mean  $TVDT_{MTS} = 40$ –67 days.

2.1.2. T1cN0-3M0. The Whole Natural History of the PT (HER2-Positive, HR(-)/HER2(+), Ki-67  $\geq 14$ ) and sdMTS

If the diameter of the PT at its resection,  $d_{PT}$ , was 15.1 mm (Figure 3; Table 1), and  $TVDT_{PT}$  was 136–165 days (intermediate growth rate of PT in patients with HR(-)/HER2(+) (HER2-positive) tumors), then the diameter of the sdMTS at PT resection,  $d_{MTS}$ , could be 0.01–1.00 mm.  $TVDT_{MTS}$  was equal to 10–135 days for rapid growth rates and/or 136–165 days for intermediate growth rates.

The total period of MTS(1-X) diagnosis may be 13.07 years (Figure 3; Table 1). BC patients with  $d_{PT} = 15.1$  mm and  $TVDT_{PT} = 136$ –165 days (T1aN0-3M0) may be considered healthy only after 13.07 years if sdMTSs were not diagnosed in this period.

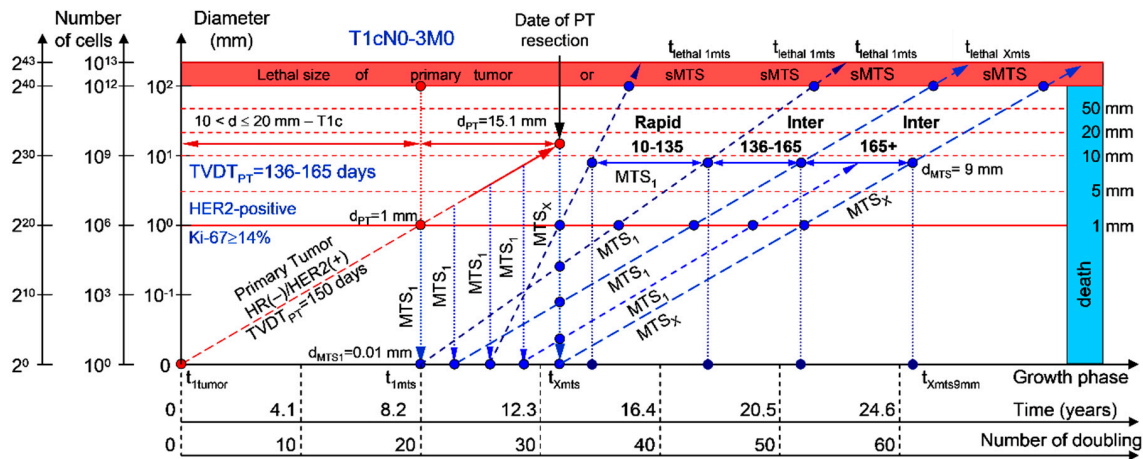


**Figure 3.** T1cN0-3M0. The whole natural history of the PT (HER2-positive, HR(-)/HER2(+), Ki-67 ≥ 14) and sdMTS. Parameter T1c: 10 mm < d ≤ 20 mm. Diameter of primary tumor =  $d_{PT} = 15.1$  mm,  $TVDT_{PT} = 136\text{--}165$  days. Rapid growth rate of secondary distant MTS =  $TVDT_{MTS} = 10\text{--}135$  days. Intermediate growth rate of secondary distant MTS =  $TVDT_{MTS} = 136\text{--}165$  days. Mean  $TVDT_{MTS} = 68\text{--}82$  days.

2.1.3. T1cN0-3M0. The Whole Natural History of the PT (Luminal B, HR(+)/HER2(-), Ki-67 ≥ 14) and sdMTS

If the diameter of the PT at its resection,  $d_{PT}$ , was 15.1 mm (Figure 4; Table 1), and the  $TVDT_{PT}$  was 166–195 days (intermediate growth rate of PT in patients with the luminal B subtype (HR(+)/HER2(-))), then the diameter of the sdMTS at the PT resection,  $d_{MTS}$ , could be 0.01–1.00 mm.  $TVDT_{MTS}$  was equal to 10–135 days for rapid growth rates, 136–165 days for intermediate growth rates, and/or 166–195 days for intermediate growth rates.

The total period of MTS(1-X) diagnosis may be 15.49 years (Figure 4; Table 1). BC patients with  $d_{PT} = 15.1$  mm and  $TVDT_{PT} = 166\text{--}195$  days (T1aN0-3M0) may be considered healthy only after 15.49 years if sdMTSs were not diagnosed in this period.

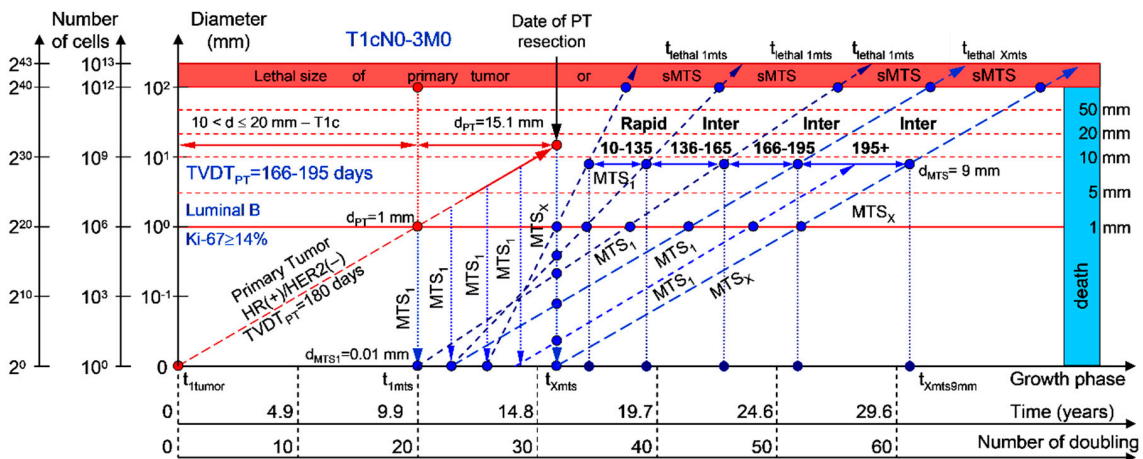


**Figure 4.** T1cN0-3M0. The whole natural history of the PT (Luminal B, HR(+)/HER2(-), Ki-67 ≥ 14) and sdMTS. Parameter T1c: 10 mm < d ≤ 20 mm. Diameter of primary tumor =  $d_{PT} = 15.1$  mm,  $TVDT_{PT} = 166\text{--}195$  days. Rapid growth rate of secondary distant MTS =  $TVDT_{MTS} = 10\text{--}135$  days. Intermediate growth rate of secondary distant MTS =  $TVDT_{MTS} = 136\text{--}195$  days. Mean  $TVDT_{MTS} = 83\text{--}97$  days.

2.1.4. T1cN0-3M0. The Whole Natural History of the PT (Luminal B, HR(+)/Her2(+), Ki-67 ≥ 14) and sdMTS

If the diameter of the PT at its resection,  $d_{PT}$ , was 15.1 mm (Figure 5; Table 1), and  $TVDT_{PT}$  was 196–230 days (slow growth rate of PT in patients with the luminal B subtype (HR(+)/HER2(+))), then the diameter of the sdMTS at PT resection,  $d_{MTS}$ , could be 0.01–1.00 mm.  $TVDT_{MTS}$  was equal to 10–135 days for rapid growth rates, 136–165 days for intermediate growth rates, 166–195 days for intermediate growth rates, and/or 196–230 days for slow growth rates.

The total period of MTS(1-X) diagnosis may be 18.32 years (Figure 5; Table 1). BC patients with  $d_{PT}$  = 15.1 mm and  $TVDT_{PT}$  = 196–230 days (T1aN0-3M0) may be considered healthy only after 18.32 years if sdMTSs were not diagnosed in this period.

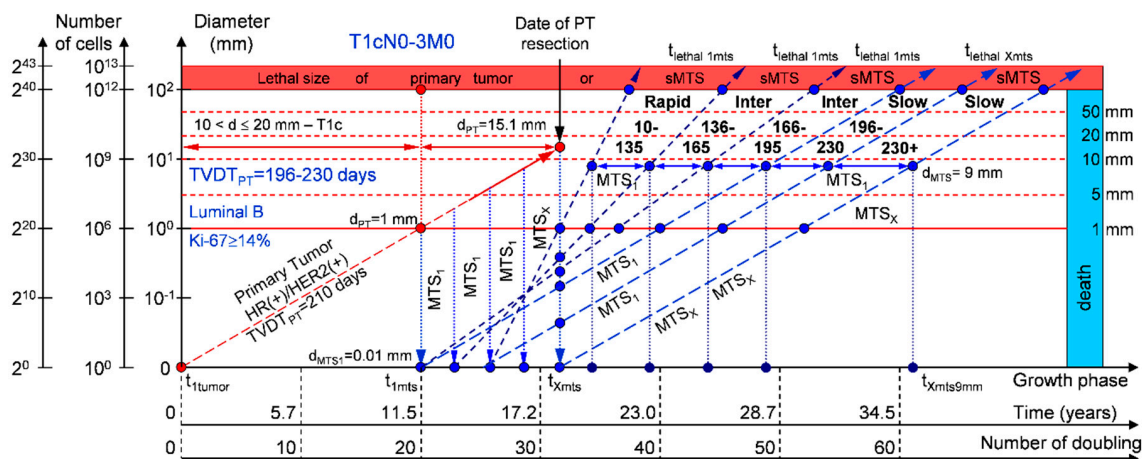


**Figure 5.** T1cN0-3M0. The whole natural history of the PT (Luminal B, HR(+)/Her2(+), Ki-67 ≥ 14) and sdMTS. Parameter T1c: 10 mm < d ≤ 20 mm. Diameter of primary tumor =  $d_{PT}$  = 15.1 mm,  $TVDT_{PT}$  = 196–230 days. Rapid growth rate of secondary distant MTS =  $TVDT_{MTS}$  = 10–135 days. Intermediate growth rate of secondary distant MTS =  $TVDT_{MTS}$  = 136–165 days. Slow growth rate of secondary distant MTS =  $TVDT_{MTS}$  = 196–230 days. Mean  $TVDT_{MTS}$  = 98–115 days.

2.1.5. T1cN0-3M0. The Whole Natural History of the PT (Luminal A, HR(+)/Her2(−), Ki-67 < 14) and sdMTS

If the diameter of the PT at its resection,  $d_{PT}$ , was 15.1 mm (Figure 6; Table 1), and  $TVDT_{PT}$  was 231–270 days (very slow growth rate of the PT in patients with the luminal A subtype (HR(+)/HER2(−))), then the diameter of the sdMTS at PT resection,  $d_{MTS}$ , could be 0.01–1.00 mm.  $TVDT_{MTS}$  was equal to 10–135 days for rapid growth rates, 136–165 days for intermediate growth rates, 166–195 days for intermediate growth rates, 196–230 days for slow growth rates, and/or 231–270 days for very slow growth rates.

The total period of MTS(1-X) diagnosis may be 12.87 years (without a 270+ period) (Figure 6; Table 1). BC patients with  $d_{PT}$  = 15.1 mm and  $TVDT_{PT}$  = 231–270 days (T1aN0-3M0) may be considered healthy only after 12.87 years if sdMTSs were not diagnosed in this period.

The CoMPaS model may help calculate the non-visible MTS-II period (MTS-free period) (Figures 2–6; Table 1). These calculated data may help define the minimal number of patient examinations in the non-visible MTS-II period (MTS-free period) depending on the growth rate of the PT and sdMTS (rapidly growing MTS, intermediately growing MTS, and slowly and very slowly growing MTS) (Figures 2–6; Table 1).

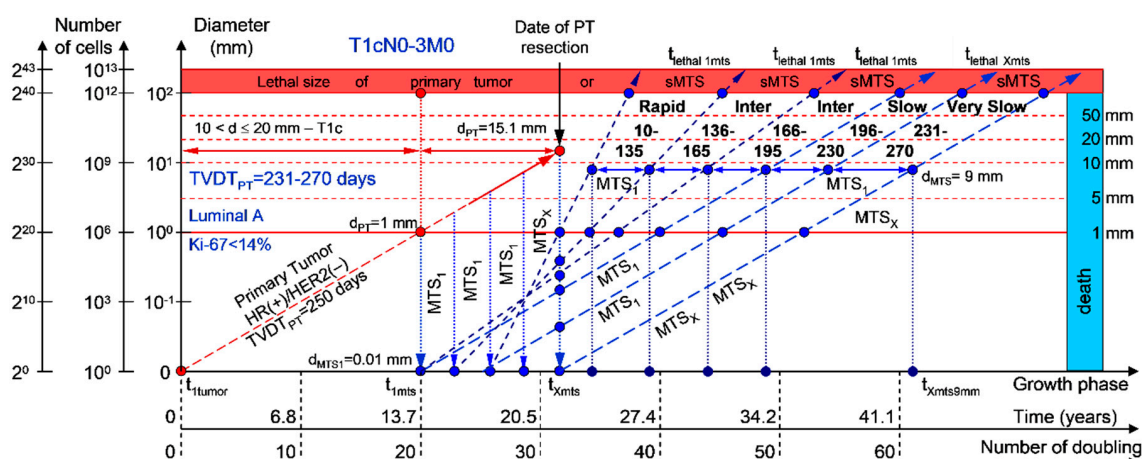


**Figure 6.** T1cN0-3M0. The *whole natural history* of the PT (Luminal A, HR(+)/Her2(-), Ki-67 < 14) and sdMTS. Parameter T1c: 10 mm < d ≤ 20 mm. Diameter of primary tumor = d<sub>PT</sub> = 15.1 mm, TVDT<sub>PT</sub> = 231–270 days. Rapid growth rate of secondary distant MTS = TVDT<sub>MTS</sub> = 10–135 days. Intermediate growth rate of secondary distant MTS = TVDT<sub>MTS</sub> = 136–166–195 days. Slow growth rate of secondary distant MTS = TVDT<sub>MTS</sub> = 196–230 days. Very slow growth rate of secondary distant MTS = TVDT<sub>MTS</sub> = 231–270 days. Mean TVDT<sub>MTS</sub> = 116–135 days.

### 2.1.6. Examinations during the MTS-Free Period

Therefore, every patient obtains personalized data on an adequate minimal number of examinations during the MTS-free period (non-visible MTS-II period). Examples are as follows:

In the period of a rapid growth rate of sdMTSs (group V with subtype V of BC—triple-negative tumors = HR(-)/HER2(-)), patients must undergo multimodal examination every three months;

In the period of an intermediate growth rate of sdMTSs (group IV with subtype V of BC—HER2-positive tumors = HR(-)/HER2(+)), patients must undergo multimodal examination every five months;

In the period of an intermediate growth rate of sdMTSs (group III with subtype III of BC—luminal B = HR(+)/HER2(-)), patients must undergo multimodal examination every six months;

In the period of a slow growth rate of sdMTSs (group II with subtype II of BC—luminal B = HR(+)/HER2(+)), patients must undergo multimodal examination every eight months;

In the period of a very slow growth rate of sdMTSs (group I with subtype I of BC—luminal A = HR(+)/HER2(-)), patients must undergo multimodal examination every nine months.

Hence, every patient obtains personalized data on an adequate maximal quantity of examinations during this period for the early diagnosis of visible sdMTSs (diameter = 5–9 mm). This may help oncologists start early treatment of small sdMTSs in BC patients (T1-3N0-3M0) and increase the survival of BC patients with sdMTSs (T1-3N0-3M0).

The CoMPaS model calculates the different diagnostic periods of sdMTS in patients with BC (T1-3N0-3M0) and facilitates the understanding of the periods of appearance and materialization of sdMTSs.

## 2.2. Application of Consolidated Mathematical Growth Model of Primary Tumor and Secondary Distant Metastases (CoMPaS) in Patients with ER/PR/HER2/Ki-67 Subtypes and Stage I/II/III Breast Cancer in Clinical Practices

This mathematical model used to predict the different diagnostic periods of sdMTS in patients with BC may help explain difficult clinical cases of BC patient survival (Figures 2–6; Table 1).

The 5–15-year survival of patients with BC depends on the diameter of the PT at resection and TVDT<sub>MTS</sub> from 10 to 270 days (Figures 2–6; Table 1).



Moreover, if patients with BC have a  $TVDT_{PT}$  from 10 to 135 days (rapid growth rate of the PT—group V with subtype V of BC—triple-negative tumors = HR(-)/HER2(-)), they have a high risk of death within five years (rapid ( $TVDT_{MTS} = 10\text{--}135$  days) growth rate of sdMTSs) (Figures 7 and 8).

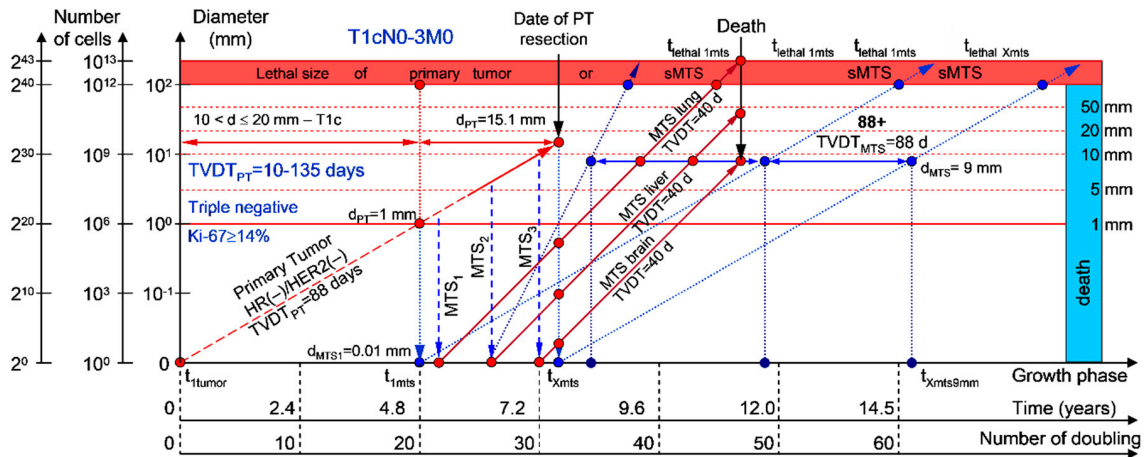


**Figure 7.** T1cN0-3M0. The whole natural history of the PT (triple-negative, HR(-)/HER2(-), Ki-67  $\geq 14$ ) and sdMTSs of patient with multiple single MTSs (lung, liver, brain). Parameter T1c:  $10\text{ mm} < d \leq 20\text{ mm}$  – T1c. Diameter of primary tumor =  $d_{PT} = 15.1\text{ mm}$ ,  $TVDT_{PT} = 88$  days. Rapid growth rate of secondary distant MTS:  $TVDT_{MTS}$  of lung metastasis = 40 days,  $TVDT_{MTS}$  of liver metastasis = 40 days,  $TVDT_{MTS}$  of brain metastasis = 40 days.

If patients with BC have a  $TVDT_{PT}$  from 136 to 165 days (intermediate growth rate of PT), they have an intermediate risk of death between five and 10 years (rapid ( $TVDT_{MTS} = 10\text{--}131$  days) and/or intermediate ( $TVDT_{MTS} = 136\text{--}165$  days) growth rate of sdMTSs).

If patients with BC have a  $TVDT_{PT}$  from 166 to 195 days (intermediate growth rate of PT), they have a low risk of death during the period from 10 to 15 years (intermediate ( $TVDT_{MTS} = 135\text{--}165$  days or  $TVDT_{MTS} = 166\text{--}195$  days) growth rate of sdMTSs).

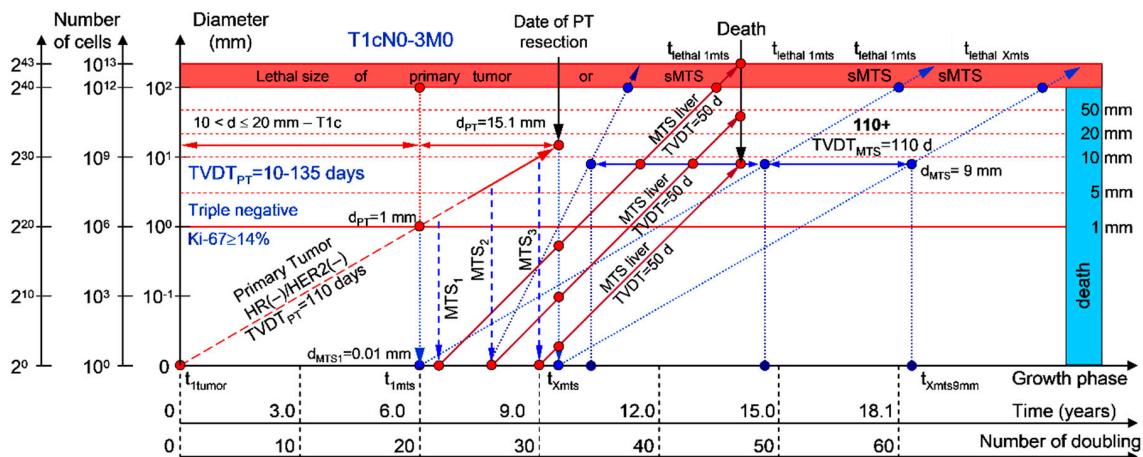


**Figure 8.** T1cN0-3M0. The whole natural history of the PT (triple-negative, HR(-)/HER2(-), Ki-67  $\geq 14$ ) and sdMTSs of patient with multiple MTSs (liver). Parameter T1c:  $10\text{ mm} < d \leq 20\text{ mm}$ . Diameter of primary tumor =  $d_{PT} = 15.1\text{ mm}$ ,  $TVDT_{PT} = 110$  days. Rapid growth rate of secondary distant MTS:  $TVDT_{MTS}$  of liver metastasis = 50 days.

If patients with BC have a  $TVDT_{PT}$  from 196 to 230 days (slow growth rate of PT), they have a low risk of death during the period from 15 to 20 years (intermediate ( $TVDT_{MTS} = 135\text{--}165$  days or  $TVDT_{MTS} = 166\text{--}195$  days) and/or slow ( $TVDT_{MTS} = 196\text{--}230$  days) growth rate of sdMTSs).

If patients with BC have a  $TVDT_{PT}$  from 231 to 270 days (very slow growth rate of PT), they have a low risk of death during the period from 20 to 25 years (intermediate ( $TVDT_{MTS} = 135\text{--}165$  days or  $TVDT_{MTS} = 166\text{--}195$  days) or slow ( $TVDT_{MTS} = 196\text{--}230$  days) or very slow ( $TVDT_{MTS} = 231\text{--}270$  days) growth rate of sdMTSs).

### 2.3. Software Tool for Personalized Scheduling of Multimodal Examinations

CoMPaS was updated with a feature that includes a recommendation to have a multimodal examination every 3–4 months  $k_1$  years after resection of the PT for  $k_2$  years. The recommendation can help oncologists assign early treatment and increase survival.

## 3. Discussion

### 3.1. The Relationship between the Size of the PT and an Appearance of the sdMTSs and TVDT

Previous studies showed that (a) the mortality rate depends directly on the PT size and (b) the risk of sdMTS appearance depends directly on the PT size [2–21,36–40,73–89].

In 2010, Holzel et al. [14] and Engel et al. [10,11,15] studied the 10- and 18-year survival from the diagnosis date to PT resection using a large patient group ( $n = 33475$ ) with regard to the BC stage (parameter T—size of the PT). It was demonstrated that the 10-year mortality linearly increases with the increasing diameter of the PT [15]. In patients with stage pT3, the 18-year mortality was higher than that in patients with stage pT2 and so forth, i.e., the 18-year mortality was much higher in patients with  $pT3 > pT2 > pT1c > pT1b > pT1a$  [14].

Hence, a larger PT results in a longer period from the determination of a visible size of the PT to the presurgery size, as well as more time for sdMTS formation before PT resection (Figure 1). In contrast, a smaller PT results in a shorter visible growth period of the PT, as well as less time for sdMTS formation before PT resection (Figure 1) [2–15,20,21,36–40,73–89].

The duration of the non-visible MTS-I period depends on the number of doublings and the TVDT [21]. According to early research results from a sequence of sdMTS appearances in BC patients after multimodal therapy, (1) a total of 75% of the recurrences were found in the first five years, (2) a total of 20% of the recurrences were found between 5–15 years, and (3) the remaining 5% of the recurrences were found in 15–25 years [20]. Therefore, the growth rate of the metastatic tumor can increase 2.2 times that of the PT; meanwhile, the TVDT can decrease 2.2 times [20].

### 3.2. The Relationship between the TVDT and the Subtypes ER/PR/HER2/Ki-67 of BC

The following observations were made: (1) BC patients with axillary lymph node MTS have a shorter TVDT than BC patients without axillary lymph node MTS ( $p < 0.05$ ); (2) BC patients positive for the estrogen receptor ER(+) in the PT have a longer TVDT than BC patients negative for the ER(−) in the PT ( $p < 0.05$ ); (3) BC patients positive for the progesterone receptor PR(+) in the PT have a longer TVDT than BC patients negative for the PR(−) in the PT ( $p < 0.05$ ); (4) BC patients negative for the Ki-67(−) receptor in the PT have a longer TVDT than BC patients positive for the Ki-67(+) receptor in the PT ( $p < 0.05$ ); (5) BC patients positive for HER2(+) in the PT have a much longer TVDT than BC patients with triple-negative HR(−)/HER2(−) expression in the PT ( $p < 0.05$ ) [52]. In other words, this study proposes that BC patients with regional lymph node MTSs have more aggressive BC and a higher risk for the appearance of sdMTSs than patients without regional lymph node MTSs who have a lower risk for the appearance of sdMTSs.

In addition, BC patients with triple-negative (HR(−)/HER2(−)) BC have more aggressive BC and a higher risk of sdMTS appearance than BC patients positive for the progesterone receptor PR(+) who have a lower risk of sdMTS appearance. Ryu et al. [49] reported the following: (1) BC patients positive for ER in the PT (ER(+)) and BC patients positive for HER2 in the PT (HER2(+)) have a much longer TVDT than BC patients with triple-negative expression in the PT ( $p < 0.05$ ).

The TVDT is one of the most critical parameters used to develop the consolidated mathematical growth model of the PT and sdMTSs of BC (CoMPaS) and to calculate the earliest diagnostic period of sdMTSs in patients with BC [21]. The TVDT, which helped in the development of the mathematical growth model, is a combined quality indicator that reflects the subtype of BC, the proliferative activity, the degree of tumor differentiation, the Nottingham prognostic index (NPI) score, receptor activity (ER(+), ER(-), PR(+), PR(-), HER2(+), HER2(-), Ki-67), and triple-negative BC [47–54,63–72,90–100]. Hence, patients can obtain a personalized approach for building a schedule of multimodal examinations to detect sdMTSs at the early stage and to start early treatment that can increase the patient's life [43].

### 3.3. The Relationship between the Different Diagnostic Periods and Subtypes ER/PR/HER2/Ki-67 of BC

Mathematical models could lead to more precise results and more meaningful prognostic risk scores, and they could integrate the planning of multimodal examinations into outcome-oriented clinical decision-making. While many useful stand-alone models are already in clinical use for forecasting the development of the BC process, the following question remains: will the patient have sdMTSs? If yes, when will the earliest period of the clinical manifestation of sdMTSs occur? If no, when will the patient be considered healthy? To answer these questions, CoMPaS was chosen as the main research tool.

Consequently, this study concentrated on calculating the different diagnostic periods (rapid growth rates in patients with triple-negative tumors (HR(-)/HER2(-)), intermediate growth rates in patients with HER2-positive tumors (HR(-)/HER2(+)), intermediate growth rates in patients with luminal B tumors (HR(+)/HER2(-)), slow growth rates in patients with luminal B tumors (HR(+)/HER2(+)), and very slow growth rates in patients with luminal A tumors (HR(+)/HER2(-)) before the manifestation of sdMTSs (MTSs) after resection of the PT. The broad implementation of the model in everyday oncology requires versatile software platforms that can be easily integrated into existing workflows and information technology (IT) architectures. Therefore, the CoMPaS model was integrated into an iOS application with input parameters such as patient data from examinations and was updated with the possibility of calculating the earliest diagnostic period.

The consolidated mathematical growth model (CoMPaS) and the corresponding software tool may be used for work with the eighth edition American Joint Committee on Cancer (AJCC) prognostic staging system for breast cancer [69–72].

If a patient has TVDT<sub>PT</sub> data, the consolidated mathematical growth model (CoMPaS) helps to calculate the data for the new personalized screening program of the sdMTS of breast cancer for each patient with T3N0-3M0 and the ER/PR/HER2/Ki-67 subtypes depending on the natural growth rate of the PT and MTS (the diagnostic periods of rapidly growing sdMTSs (HR(-)/HER2(-)—triple-negative tumors), intermediately growing sdMTSs (HR(-)/HER2(+)—HER2-positive tumors), intermediately growing sdMTSs (luminal B = HR(+)/HER2(-)), slowly growing sdMTSs (luminal B = HR(+)/HER2(+)), and very slowly growing sdMTSs (luminal A = HR(+)/HER2(-))) (Figures 1–8; Table 1) [22,23,69–72,101–106].

### 3.4. The Relationship between the Mortality and the Convalescence and Subtypes ER/PR/HER2/Ki-67 of BC

In patients with triple-negative tumors (HR(-)/HER2(-)), the five-year mortality was higher than that in patients with HER2-positive tumors (HR(-)/HER2(+)) and so forth, i.e., the five-year mortality was much higher in patients with triple-negative tumors (HR(-)/HER2(-)) > patients HER2-positive tumors (HR(-)/HER2(+)) > patients with luminal B subtype tumors (HR(+)/HER2(-)) > patients with luminal B subtype tumors (HR(+)/HER2(+)) > patients with luminal A subtype tumors (HR(+)/HER2(-)) [22–26,69–72,101–106].

Moreover, if sdMTSs did not appear in the different diagnostic periods (rapid growth rate in patients with triple-negative tumors (HR(-)/HER2(-)), intermediate growth rate in patients with HER2-positive tumors (HR(-)/HER2(+)), intermediate growth rate in patients with luminal B subtype tumors (HR(+)/HER2(-)), slow growth rate in patients with luminal B subtype tumors (HR(+)/HER2(+)),

and very slow growth rate in patients with luminal A subtype tumors (HR(+)/HER2(-)), the patient could be considered to be almost healthy, and she could be classified into the survival group. The consolidated mathematical growth model of the PT and sdMTSs of BC (CoMPaS) can calculate the total period of MTS(1-X) diagnosis and determine the time when patients may be considered healthy (Figures 1–8; Table 1).

As a consequence, oncologists can determine the causes of BC appearance considering the knowledge of when the first tumor cell appeared, which can lead to the development of prevention methods. The relationship between the PT and sdMTSs can provide a deeper understanding of the BC process [2–15,20,21,36–41,73–89]. The calculation of the earliest diagnostic period can help with the assignment of early treatment and increase survival [82–89,100]. Clinics can plan procedures with optimal usage of resources and an understanding of when a patient will come to the hospital.

#### 4. Materials and Methods

##### 4.1. Consolidated Mathematical Growth Model of Primary Tumor and Secondary Distant Metastases (CoMPaS)

To describe the growth processes of PTs and sdMTSs at stages I and II, the CoMPaS model was developed. A detailed description and the limitations of CoMPaS, as well as the influence of the appearance of the first sdMTS on the survival prognosis of a patient, were provided previously. Figure 1 demonstrates the model in terms of the whole natural history of PT and sdMTS growth [21].

The whole natural growth history of the PT and sdMTSs includes the non-visible growth period of the PT, the visible growth period of the PT, the non-visible growth period of the sdMTSs, and the visible growth period of the sdMTSs [21]. The non-visible period of PT growth is from the appearance of the first tumor cell (diameter = 10  $\mu\text{m}$ ) until it reaches a visible size (diameter = 1–5 mm) [21]. The visible period of PT growth is from the time that it reaches a visible size (diameter = 1–5 mm) up to the time that it reaches pre-surgery size. The non-visible period of MTS growth can be calculated as the period from diagnosis (date of PT resection) to the time that at least one MTS reaches a visible size (diameter = 1–5 mm) [21]. The visible period of MTS growth can be calculated as the period from diagnosis of the visible size (diameter = 1–5 mm) to when it reaches lethal size (death) [21]. Thus, descriptions of the whole natural history of BC require building a consolidated mathematical BC growth model of the PT and secondary distant MTSs [21].

The following updated formulas illustrate the mathematical side of the CoMPaS [21]:

$$\frac{dV}{dt} = \frac{\log 2}{DT} V, t \leq DT \quad \log 2 \left( \theta \frac{DT}{\log 2} \right) V_0, \quad (1)$$

$$\frac{dV}{dt} = \theta \log V, t > DT \quad \log_2 \left( \theta \frac{DT}{\log 2} V_0 \right), \quad (2)$$

$$V(t = 0) = V_0,$$

$$60 = \log 2^{N_{pt}} + \log 2^{N_{mtsII}} + \log 2^{N_{mtsII-vis}}, \quad (3)$$

$$TVDT_{non} = TVDT_{vis} = \frac{\log 2_{days}^{N_{mtsII}} + \log 2_{days}^{N_{mtsII-vis}}}{\log 2^{N_{mtsII}} + \log 2^{N_{mtsII-vis}}}, \quad (4)$$

where  $\frac{\log 2}{DT}$  is the fraction of proliferative cell times,  $\theta$  drives the linear phase ( $\theta = 1$ ),  $N_{pt}$  is the number of PT doublings,  $N_{mtsII}$  is the number of doublings for the *non-visible* growth period of sdMTS,  $N_{mts-vis}$  is the number of doublings for the *visible* growth period of sdMTS,  $TVDT$  is the tumor volume doubling time, and 60 doublings represent the *whole nature growth history* of the PT and sdMTSs.

CoMPaS is based on an exponential growth model that consists of nonlinear and linear deterministic equations [21]. Available studies based on clinical data demonstrate exponential PT growth in patients with BC [36–39,44–47]. The growth rate of the PT in patients with BC is calculated via

$TVDT_{PT}$  [36–39,44–47]. An ultrasound-based diagnosis allows a better detection of the changes in PT sizes in patients with BC to calculate  $TVDT_{PT}$  [48–54].

The appearance of the first metastatic cell of the first sdMTS coincides with the 20th doubling of the PT of BC, which allows defining the non-visible growth period of the sdMTS and the initial period of sdMTS manifestation [7,14,15,21,55,56]. The appearance of the last metastatic cell of sdMTS coincides with the date of BC PT resection [21].

Available studies based on clinical data demonstrate exponential sdMTS growth between 1 mm and 60 mm in patients with BC [20,21,55–62]. The growth rate of sdMTSs in patients with BC is calculated via  $TVDT_{MTS}$  [57–62]. An ultrasound diagnosis allows a better detection of the changes in sdMTS sizes (liver, subcutaneous MTSs) in patients with BC to calculate  $TVDT_{PT}$  [48–54]. A computed tomography (CT) scan and magnetic resonance imaging (MRI) scan also allow a better detection of the changes in sdMTS sizes (lungs, brain) in patients with BC to calculate  $TVDT_{PT}$  [48–54].

The growth rate of sdMTSs in patients with BC ( $TVDT_{MTS}$ ) may correspond to (equal) the growth rate of the PT ( $TVDT_{PT}$ ) or may be 2–2.2-times higher [2–7,55,56]. The growth rate of secondary distant MTSs may be a rapid growth rate, an intermediate growth rate, or a slow growth rate [2–4,6,7]. The growth rate of the PT and sdMTSs in patients with BC can determine the survival forecast of these patients [2–7,41,42,62–68].

The model describes the following: (a) PT growth from 1 mm up to 60 mm (exponential growth of the PT) without/with MTSs in the lymph nodes; (b) a  $TVDT_{PT}$  from 10 days to 310 days; (c) sdMTSs growth from 1 mm up to 60 mm (exponential growth of the sdMTSs); (d) a  $TVDT_{MTS}$  from 10 days to 310 days.  $TVDT_{MTS}$  must be bigger than 10 days, but  $TVDT_{MTS}$  must be less than or equal to  $TVDT_{PT}$ .

#### 4.2. A Mathematical Model to Predict the Earliest Diagnostic Periods of Secondary Distant Metastases in Patients with ER/PR/HER2/Ki-67 Subtypes of Breast Cancer

The growth period of sdMTSs includes the non-visible growth period of sdMTSs, the visible growth period of sdMTSs, diagnostics, treatment, and patient death [21]. The non-visible growth period of sdMTSs consists of two periods: (1) the non-visible growth period of the sdMTS from the appearance of the first metastatic cell of the sdMTS to the date of PT resection (non-visible sdMTS(1)-I), and (2) the non-visible growth period of the sdMTS from the diagnosis (the date of PT resection) to the time when the visible size of at least one sdMTS can be diagnosed (non-visible MTS(1)-II) (Figure 1). It should be noted that the non-visible growth period of sdMTS(1)-II is described as the MTS-free period in other papers.

It is difficult to predict which metastatic cell (from the PT: 1 mm, 2 mm or 3 mm) will be the initial point of sdMTS growth (Figure 1). Considering prior assumptions, it is relevant to set the initial point as the *non-visible MTS(1-X) (years)* and the progression as the *Period of MTS(1-X) diagnosis* for the critical periods of the *earliest diagnosis* of the sdMTS (Figure 1).

The *natural* growth rate of the sdMTS may be similar to the *natural* growth rate of the PT of BC (Figure 1).

PTs of breast cancer were divided into five different groups depending on the ER/PR/HER2/Ki-67 subtypes and growth rates [49,50,52–54]:

Group I with a very slow growth rate of the PT, with subtype I of BC—luminal A = HR(+)/HER2(–) for HR-positive (ER+/PR+, ER+/PR–, or ER–/PR+) tumors, Ki-67 < 14% ( $TVDT_{PT}$  = 231–270 days);

Group II with a slow growth rate of the PT, with subtype II of BC—luminal B = HR(+)/HER2(+) for HR-positive (ER+/PR+, ER+/PR–, or ER–/PR+) and Her2-positive tumors, Ki-67 ≥ 14% ( $TVDT_{PT}$  = 196–230 days);

Group III with an intermediate growth rate of the PT, with subtype III of BC—luminal B = HR(+)/HER2(–) for HR-positive (ER+/PR+ or ER+/PR– or ER–/PR+) tumors, Ki-67 ≥ 14% ( $TVDT_{PT}$  = 166–195 days);

Group IV with an intermediate growth rate of the PT, with subtype IV of BC—HR(–)/HER2(+) for HER2-positive tumors, Ki-67 ≥ 14% ( $TVDT_{PT}$  = 136–165 days);

Group V with a rapid growth rate of the PT with subtype V of BC—HR(−)/HER2(−) for triple-negative tumors, Ki-67  $\geq$  14% (TVDT<sub>PT</sub> = 10–135 days).

However, the growth rate of the secondary distant MTS may be higher than the *natural* growth rate of the BC PT [2–4,6,7]. For the first time, the growth rates of secondary distant MTSs were divided into five groups depending on the ER/PR/HER2/Ki-67 subtypes and growth rates [49,50,52–54]: group I with subtype I of BC (luminal A = HR(+)/HER2(−)) for sdMTSs with very slow growth rates (TVDT<sub>MTS</sub> = 231–270 days), group II with subtype II of BC (luminal B = HR(+)/HER2(+)) for sdMTSs with slow growth rates (TVDT<sub>MTS</sub> = 196–230 days), group III with subtype III of BC (luminal B = HR(+)/HER2(−)) for sdMTSs with intermediate growth rates (TVDT<sub>MTS</sub> = 166–195 days), group IV with subtype IV of BC (HR(−)/HER2(+))—HER2-positive tumors for sdMTSs with intermediate growth rates (TVDT<sub>MTS</sub> = 136–165 days), and group V with subtype V (HR(−)/HER2(−))—triple-negative tumors of BC for sdMTSs with rapid growth rates (TVDT<sub>MTS</sub> = 10–135 days) [2–4,6,7,20,22–26,40,47,49,52–54,69–72].

#### 4.3. Limitations

The model does not describe or explain an appearance of the secondary distant MTSs (M1) in patients with stage T4N0-3M0.

#### 4.4. Implementation Software

The application was built using Swift and references CoMPaS, where the input data consist of the following fields that a user (doctor) must fill: the *first* diagnostic data (date of diagnostics, diameter of the PT in mm) and the *second* diagnostic data (date of diagnostics, diameter of the PT in mm, subtype). As a result, the output data provide the following: prognosis (the *category* of prognosis: favorable, mid-favorable, unfavorable; the *number of months* before the manifestation of the sdMTSs) [21].

#### 4.5. Calculation Method

The obtained results were calculated on a personal computer (PC) using Python 3.8.

### 5. Conclusions

The implementation of CoMPaS and the corresponding software tool offers fascinating prospects for personalized diagnostics and early treatment by detecting the earliest diagnostic period of sdMTSs in BC patients (T1-3N0-3M0 and ER/PR/HER2/Ki-67 subtypes) with regard to the eighth edition AJCC prognostic staging system for breast cancer and the growth rate of the PT and sdMTSs in BC [22–26,69–72,101–106]. Such mathematics-based approaches could better identify high-risk patients in the future and help prevent unnecessary treatments. Therefore, this approach could integrate diagnostic oncology more closely with outcome-oriented clinical decisions by increasing the survival of BC patients with sdMTSs (T1-3N0-3M0 and ER/PR/HER2/Ki-67 subtypes). These kinds of gains in efficiency will become increasingly important, given the growing demand for less toxic treatments and the discovery of almost healthy patients.

### 6. Patents

The predictor of the whole natural history of breast cancer (COMBREC): Certificate of the state registration of the computer program No. 2018612104. Date of the state registration in the register of computer programs: 12.02.2018. Authors: Neznanov AA, Tyuryumina EYa.

**Author Contributions:** Conceptualization, E.Y.T.; methodology, E.Y.T., A.A.N., and J.L.T.; software, E.Y.T.; validation, J.L.T.; formal analysis, A.A.N.; investigation, E.Y.T., A.A.N., and J.L.T.; resources, A.A.N.; data curation, E.Y.T. and A.A.N.; writing—original draft preparation, E.Y.T.; writing—review and editing, E.Y.T., A.A.N., and J.L.T.; visualization, E.Y.T.; supervision, A.A.N. and J.L.T.; project administration, E.Y.T.; funding acquisition, A.A.N. All authors read and agreed to the published version of the manuscript.

**Funding:** The article/book/book chapter was prepared within the framework of the HSE University Basic Research Program and funded by the Russian Academic Excellence Project “5–100”.

**Conflicts of Interest:** The authors declare no conflict of interest.

## References

1. Shah, R.; Rosso, K.; Nathanson, S.D. Pathogenesis, prevention, diagnosis and treatment of breast cancer. *World J. Clin. Oncol.* **2014**, *5*, 283–298. [[CrossRef](#)] [[PubMed](#)]
2. Slack, N.H.; Blumenson, L.E.; Bross, I.D. Therapeutic implications from a mathematical model characterizing the course of breast cancer. *Cancer* **1969**, *24*, 960–971. [[CrossRef](#)]
3. Pearlman, A.W. Breast cancer: Influence of growth rate on prognosis and treatment evaluation. *Cancer* **1976**, *38*, 1826–1833. [[CrossRef](#)]
4. Koscielny, S.; Tubiana, M.; Valleron, A.-J. A simulation model of the natural history of human breast cancer. *Br. J. Cancer.* **1985**, *52*, 515–524. [[CrossRef](#)]
5. Koscielny, S.; Le, M.G.; Tubiana, M. The natural history of human breast cancer. The relationship between involvement of axillary lymph nodes and the initiation of distant metastases. *Br. J. Cancer.* **1989**, *59*, 775–782. [[CrossRef](#)]
6. Tubiana, M.; Courdi, A. Cell proliferation kinetics in human solid tumors: Relation to probability of metastatic dissemination and long-term survival. *Radiother. Oncol.* **1989**, *15*, 1–18. [[CrossRef](#)]
7. Friberg, S.; Mattson, S. On the growth rates of human malignant tumors: Implications for medical decision making. *J. Surg. Oncol.* **1997**, *65*, 284–297. [[CrossRef](#)]
8. Michaelson, J.S.; Silverstein, M.; Wyatt, J.; Weber, G.; Moore, R.; Halpern, E.; Kopans, D.B.; Hughes, K. Predicting the survival of patients with breast carcinoma using tumor size. *Cancer* **2002**, *95*, 713–723. [[CrossRef](#)]
9. Michaelson, J.S.; Silverstein, M.; Sgroi, D.; Cheongsiatmoy, J.A.; Taghian, A.; Powell, S.; Hughes, K.; Comegno, A.; Tanabe, K.K.; Smith, B. The effect of tumor size and lymph node status on breast carcinoma lethality. *Cancer* **2003**, *98*, 2133–2143. [[CrossRef](#)]
10. Engel, J.; Eckel, R.; Aydemir, U.; Aydemir, S.; Kerr, J.; Schlesinger-Raab, A.; Dirschedl, P.; Hölzel, D. Determinants and prognoses of locoregional and distant progression in breast cancer. *Int. J. Radiat. Oncol. Biol. Phys.* **2003**, *55*, 1186–1195. [[CrossRef](#)]
11. Engel, J.; Eckel, R.; Kerr, J.; Schmidt, M.; Fürstenberger, G.; Richter, R.; Sauer, H.; Senn, H.J.; Hölzel, D. The process of metastasisation for breast cancer. *Eur. J. Cancer* **2003**, *39*, 1794–1806. [[CrossRef](#)]
12. Klein, C.A.; Hölzel, D. Systemic cancer progression and tumor dormancy: Mathematical models meet single cell genomics. *Cell Cycle* **2006**, *5*, 1788–1798. [[CrossRef](#)] [[PubMed](#)]
13. Michaelson, J.S.; Chen, L.L.; Silverstein, M.J.; Cheongsiatmoy, J.A.; Mihm, M.C., Jr.; Sober, A.J.; Tanabe, K.K.; Smith, B.L.; Younger, J. Why cancer at primary site and in the lymph nodes contributes to the risk of cancer death. *Cancer* **2009**, *115*, 5084–5094. [[CrossRef](#)]
14. Hölzel, D.; Eckel, R.; Emeny, R.T.; Engel, J. Distant metastases do not metastasize. *Cancer Metastasis Rev.* **2010**, *29*, 737–750. [[CrossRef](#)] [[PubMed](#)]
15. Engel, J.; Emeny, R.T.; Hölzel, D. Positive lymph nodes do not metastasize. *Cancer Metastasis Rev.* **2012**, *31*, 235–246. [[CrossRef](#)] [[PubMed](#)]
16. Clare, S.E.; Nakhli, F.; Panetta, J.C. Molecular biology of breast cancer metastasis: The use of mathematical models to determine relapse and to predict response to chemotherapy in breast cancer. *Breast Cancer Res.* **2000**, *2*, 430–435. [[CrossRef](#)]
17. Withers, H.R.; Lee, S.P. Modeling growth kinetics and statistical distribution of oligometastases. *Semin. Radiat. Oncol.* **2006**, *16*, 111–119. [[CrossRef](#)]
18. Weedon-Fekjaer, H.; Lindqvist, B.H.; Vatten, L.J.; Aalen, O.O.; Tretli, S. Breast cancer tumor growth estimated through mammography screening data. *Breast Cancer Res.* **2008**, *10*, R41. [[CrossRef](#)]
19. Molina-Pena, R.; Alvarez, M.M. A simple mathematical model based on the cancer stem cell hypothesis suggests kinetic commonalities in solid tumor growth. *PLoS ONE* **2012**, *7*, e26233. [[CrossRef](#)]
20. Coumans, F.A.; Siesling, S.; Terstappen, L.W. Detection of cancer before distant metastases. *BMC Cancer* **2013**, *13*, 283. [[CrossRef](#)]
21. Tyuryumina, E.; Neznanov, A. Consolidated mathematical growth model of the primary tumor and sdMTS of breast cancer (CoMPaS). *PLoS ONE* **2018**, *13*, e0200148. [[CrossRef](#)] [[PubMed](#)]

22. Parise, C.A.; Caggiano, V. Breast cancer survival defined by the ER/PR/HER2 subtypes and a surrogate classification according to tumor grade and immunohistochemical biomarkers. *J. Cancer Epidemiol.* **2014**, *2014*, 469251. [[CrossRef](#)] [[PubMed](#)]
23. Chavez-MacGregor, M.; Mittendorf, E.A.; Clarke, C.A.; Lichtensztajn, D.Y.; Hunt, K.K.; Giordano, S.H. Incorporating tumor characteristics to the American joint committee on cancer breast cancer staging system. *Oncologist* **2017**, *22*, 1292–1300. [[CrossRef](#)] [[PubMed](#)]
24. Howlader, N.; Cronin, K.A.; Kurian, A.W.; Andridge, R. Differences in breast cancer survival by molecular subtypes in the United States. *Cancer Epidemiol. Biomark. Prev.* **2018**, *27*, 619–626. [[CrossRef](#)]
25. Harbeck, N.; Penault-Llorca, F.; Cortes, J.; Gnant, M.; Houssami, N.; Poortmans, P.; Ruddy, K.; Tsang, J.; Cardoso, F. Breast cancer. *Nat. Rev. Dis. Primers* **2019**, *5*, 66. [[CrossRef](#)]
26. Lawrenson, R.; Lao, C.; Campbell, I.; Harvey, V.; Seneviratne, S.; Elwood, M.; Sarfati, D.; Kuper-Hommel, M. The impact of different tumor subtypes on management and survival of New Zealand women with stage I-III breast cancer. *N. Z. Med. J.* **2018**, *131*, 51–60.
27. Lafranconi, A.; Pylkkanen, L.; Deandrea, S.; Bramesfeld, A.; Lerda, D.; Neamtiu, L.; Saz-Parkinson, Z.; Posso, M.; Rigau, D.; Sola, I.; et al. Intensive follow-up for women with breast cancer: Review of clinical, economic and patient's preference domains through evidence to decision framework. *Health Qual. Life Outcomes* **2017**, *15*, 206. [[CrossRef](#)]
28. Smith, T.J. Breast cancer surveillance guidelines. *J. Oncol. Pract.* **2013**, *9*, 65–67. [[CrossRef](#)]
29. Puglisi, F.; Fontanella, C.; Numico, G.; Sini, V.; Evangelista, L.; Monetti, F.; Gori, S.; Del Mastro, L. Follow-up of patients with early breast cancer: Is it time to rewrite the story? *Crit. Rev. Oncol. Hematol.* **2014**, *91*, 130–141. [[CrossRef](#)]
30. Stevens, G.M.; Weigen, J.F. Mammography survey for breast cancer detection. A 2-year study of 1,223 clinically negative asymptomatic women over 40. *Cancer.* **1966**, *19*, 51–59. [[CrossRef](#)]
31. Khatcheressian, J.L.; Wolff, A.C.; Smith, T.J.; Grunfeld, E.; Muss, H.B.; Vogel, V.G.; Halberg, F.; Somerfield, M.R.; Davidson, N.E. American Society of Clinical Oncology 2006 updates of the breast cancer follow-up and management guidelines in the adjuvant setting. *J. Clin. Oncol.* **2006**, *24*, 5091–5097. [[CrossRef](#)] [[PubMed](#)]
32. Khatcheressian, J.L.; Hurley, P.; Bantug, E.; Esserman, L.J.; Grunfeld, E.; Halberg, F.; Hantel, A.; Henry, N.L.; Muss, H.B.; Smith, T.J.; et al. Breast cancer follow-up and management after primary treatment: American Society of Clinical Oncology clinical practice guideline update. *J. Clin. Oncol.* **2013**, *31*, 961–965. [[CrossRef](#)] [[PubMed](#)]
33. Collins, V.P.; Loeffler, R.K.; Tivey, H. Observations on growth rates of human tumors. *Am. J. Roentgen.* **1956**, *76*, 988–1000.
34. Schwartz, M. A biomathematical approach to clinical tumor growth. *Cancer* **1961**, *14*, 1272–1294. [[CrossRef](#)]
35. Bloom, H.J.; Richarson, W.W.; Harries, E.J. Natural history of untreated breast cancer (1805–1933). Comparison of untreated and treated cases according to histological grade of malignancy. *Br. Med. J.* **1962**, *2*, 213–221. [[CrossRef](#)] [[PubMed](#)]
36. Skipper, H.E. Kinetics of mammary tumor cell growth and implications for therapy. *Cancer* **1971**, *28*, 1479–1499. [[CrossRef](#)]
37. Silvestrini, R.; Sanfilippo, O.; Tedesco, G. Kinetics of human mammary carcinomas and their correlation with the cancer and the host characteristics. *Cancer* **1974**, *34*, 1252–1258. [[CrossRef](#)]
38. Lundgren, B. Observations on growth rate of breast carcinomas and its possible implications for lead time. *Cancer* **1977**, *40*, 1722–1725. [[CrossRef](#)]
39. Spratt, J.A.; von Fournier, D.; Spratt, J.S.; Weber, E.E. Mammographic assessment of human breast cancer growth and duration. *Cancer* **1993**, *71*, 2020–2026. [[CrossRef](#)]
40. Moiseenko, V.M. The natural history of breast cancer growth. *Pract. Oncol.* **2002**, *3*, 6–14. (In Russian)
41. Rodriguez-Brenes, I.A.; Komarova, N.L.; Wodarz, D. Tumor growth dynamics: Insights into evolutionary processes. *Trends Ecol. Evol.* **2013**, *28*, 597–604. [[CrossRef](#)] [[PubMed](#)]
42. Benzekry, S.; Lamont, C.; Beheshti, A.; Tracz, A.; Ebos, J.M.; Hlatky, L.; Hahnfeldt, P. Classical mathematical models for description and prediction of experimental tumor growth. *PLoS Comput. Biol.* **2014**, *10*, e1003800. [[CrossRef](#)] [[PubMed](#)]



43. Wu, X.; Ye, Y.; Barcenas, C.H.; Chow, W.H.; Meng, Q.H.; Chavez-MacGregor, M.; Hildebrandt, M.A.; Zhao, H.; Gu, X.; Deng, Y.; et al. Personalized prognostic prediction models for breast cancer recurrence and survival incorporating multidimensional data. *J. Natl. Cancer Inst.* **2017**, *109*, djw314. [[CrossRef](#)] [[PubMed](#)]
44. Gershon-Cohen, J.; Berger, S.M.; Klickstein, H.S. Roentgenography of breast cancer moderating concept of “Biologic predeterminism”. *Cancer* **1963**, *16*, 961–964. [[CrossRef](#)]
45. Kusama, S.; Spratt, J.S., Jr.; Donegan, W.L.; Watson, F.R.; Cunningham, C. The cross rates of growth of human mammary carcinoma. *Cancer* **1972**, *30*, 594–599. [[CrossRef](#)]
46. von Fournier, D.V.; Weber, E.; Hoeffken, W.; Bauer, M.; Kubli, F.; Barth, V. Growth rate of 147 mammary carcinomas. *Cancer* **1980**, *45*, 2198–2207. [[CrossRef](#)]
47. Peer, P.G.; van Dijck, J.A.; Hendriks, J.H.; Holland, R.; Verbeek, A.L. Age-dependent growth rate of primary breast cancer. *Cancer* **1993**, *71*, 3547–3551. [[CrossRef](#)]
48. Gruber, I.V.; Rueckert, M.; Kagan, K.O.; Staebler, A.; Siegmann, K.C.; Hartkopf, A.; Wallwiener, D.; Hahn, M. Measurement of tumor size with mammography, sonography and magnetic resonance imaging as compared to histological tumor size in primary breast cancer. *BMC Cancer* **2013**, *13*, 328. [[CrossRef](#)]
49. Ryu, E.B.; Chang, J.M.; Seo, M.; Kim, S.A.; Lim, J.H.; Moon, W.K. Tumor volume doubling time of molecular breast cancer subtypes assessed by serial breast ultrasound. *Eur. Radiol.* **2014**, *24*, 2227–2235. [[CrossRef](#)]
50. Yoo, T.K.; Min, J.W.; Kim, M.K.; Lee, E.; Kim, J.; Lee, H.B.; Kang, Y.J.; Kim, Y.G.; Moon, H.G.; Moon, W.K.; et al. In vivo tumor growth rate measured by US in preoperative period and long term disease outcome in breast cancer patients. *PLoS ONE* **2015**, *10*, e0144144. [[CrossRef](#)]
51. Cortadellas, T.; Argacha, P.; Acosta, J.; Rabasa, J.; Peiró, R.; Gomez, M.; Rodellar, L.; Gomez, S.; Navarro-Golobart, A.; Sanchez-Mendez, S.; et al. Estimation of tumor size in breast cancer comparing clinical examination, mammography, ultrasound and MRI—correlation with the pathological analysis of the surgical specimen. *Gland Surg.* **2017**, *6*, 330–335. [[CrossRef](#)] [[PubMed](#)]
52. Zhang, S.; Ding, Y.; Zhou, Q.; Wang, C.; Wu, P.; Dong, J. Correlation factors analysis of breast cancer tumor volume doubling time measured by 3D-Ultrasound. *Med. Sci. Monit.* **2017**, *23*, 3147–3153. [[CrossRef](#)] [[PubMed](#)]
53. Nakashima, K.; Uematsu, T.; Takahashi, K.; Nishimura, S.; Tadokoro, Y.; Hayashi, T.; Sugino, T. Does breast cancer growth rate really depend on tumor subtype? Measurement of tumor doubling time using serial ultrasonography between diagnosis and surgery. *Breast Cancer* **2019**, *26*, 206–214. [[CrossRef](#)] [[PubMed](#)]
54. Lee, S.H.; Kim, Y.S.; Han, W.; Ryu, H.S.; Chang, J.M.; Cho, N.; Moon, W.K. Tumor growth rate of invasive breast cancers during wait times for surgery assessed by ultrasonography. *Medicine (Baltim.)* **2016**, *95*, e4874. [[CrossRef](#)] [[PubMed](#)]
55. Friberg, S. On the growth rates of human malignant tumors: Implications for medical decision making. *J. Oncol.* **2005**, *55*, 1–22.
56. Klein, C.A. Parallel progression of primary tumors and metastases. *Nat. Rev. Cancer.* **2009**, *9*, 302–312. [[CrossRef](#)]
57. Spratt, J.S.; Spratt, T.L. Rates of growth of pulmonary metastases and host survival. *Ann. Surg.* **1964**, *159*, 61–171. [[CrossRef](#)]
58. Philippe, E.; Le Gal, Y. Growth of 78 recurrent mammary cancers. *Cancer* **1968**, *21*, 461–467. [[CrossRef](#)]
59. Lee, Y.T.; Spratt, J.S., Jr. Rate of growth of soft tissue metastases of breast cancer. *Cancer* **1972**, *29*, 344–348. [[CrossRef](#)]
60. Gullino, P.M. Natural history of breast cancer. Progression from hyperplasia to neoplasia as predicted by angiogenesis. *Cancer* **1977**, *39*, 2697–2703. [[CrossRef](#)]
61. Retsky, M.W.; Swartzendruber, D.E.; Wardwell, R.H.; Bame, P.D. Is Gompertzian or exponential kinetics a valid description of individual human cancer growth? *Med. Hypotheses* **1990**, *33*, 95–106. [[CrossRef](#)]
62. Spratt, J.S.; Kaltenbach, M.L.; Spratt, J.A. Cytokinetic definition of acute and chronic breast cancer. *Cancer Res.* **1977**, *37*, 226–230. [[PubMed](#)]
63. Boyd, N.F.; Meakin, J.W.; Hayward, J.L.; Brown, T.C. Clinical estimation of the growth rate of breast cancer. *Cancer* **1981**, *48*, 1037–1042. [[CrossRef](#)]
64. Galante, E.; Gallus, G.; Guzzon, A.; Bono, A.; Bandieramonte, G.; Di Pietro, S. Growth rate of primary breast cancer and prognosis: Observations on a 3- to 7-year follow-up in 180 breast cancers. *Br. J. Cancer.* **1986**, *54*, 833–836. [[CrossRef](#)] [[PubMed](#)]

65. Kuroishi, T.; Tominaga, S.; Morimoto, T.; Tashiro, H.; Itoh, S.; Watanabe, H.; Fukuda, M.; Ota, J.; Horino, T.; Ishida, T.; et al. Tumor growth rate and prognosis of breast cancer mainly detected by mass screening. *Jpn. J. Cancer Res.* **1990**, *81*, 454–462. [[CrossRef](#)]
66. Spratt, J.A.; von Fournier, D.; Spratt, J.S.; Weber, E.E. Decelerating growth and human breast cancer. *Cancer* **1993**, *71*, 2013–2019. [[CrossRef](#)]
67. Friberg, S.; Nyström, A. Cancer metastases: Early dissemination and late recurrences. *Cancer Growth Metastasis* **2015**, *8*, 43–49. [[CrossRef](#)]
68. Tabbane, F.; Bahi, J.; Rahal, K.; May, A.E.; Riahi, M.; Cammoun, M.; Hechiche, M.; Jaziri, M.; Mourali, N. Inflammatory symptoms in breast cancer. Correlations with growth rate, clinicopathologic variables, and evolution. *Cancer* **1989**, *64*, 2081–2089. [[CrossRef](#)]
69. Hortobagyi, G.; Connolly, J.L.; D’Orsi, C.J.; Edge, S.B.; Mittendorf, E.A.; Rugo, H.S.; Solin, L.J.; Weaver, D.L.; Winchester, D.J.; Giuliano, A. Breast. In *AJCC Cancer Staging Manual*, 8th ed.; Amin, M.B., Edge, S., Greene, F., Byrd, D.R., Brookland, R.K., Washington, M.K., Gershenwald, J.E., Compton, C.C., Hess, K.R., Sullivan, D.C., et al., Eds.; American Joint Committee on Cancer (AJCC): New York, NY, USA; Springer: Berlin/Heidelberg, Germany, 2017; pp. 587–628. ISBN 978-3-319-40617-6. [[CrossRef](#)]
70. Hortobagyi, G.N.; Edge, S.B.; Giuliano, A. New and important changes in the TNM staging system for breast cancer. *Am. Soc. Clin. Oncol. Educ. Book* **2018**, *38*, 457–467. [[CrossRef](#)]
71. Zhang, J.; Zhao, B.; Jin, F. The assessment of 8th edition AJCC prognostic staging system and a simplified staging system for breast cancer: The analytic results from the SEER database. *Breast J.* **2019**, *25*, 838–847. [[CrossRef](#)]
72. He, J.; Tsang, J.Y.; Xu, X.; Li, J.; Li, M.; Chao, X.; Xu, Y.; Luo, R.; Tse, G.M.; Sun, P. AJCC 8th edition prognostic staging provides no better discriminatory ability in prognosis than anatomical staging in triple negative breast cancer. *BMC Cancer* **2020**, *20*, 18. [[CrossRef](#)] [[PubMed](#)]
73. Koscielny, S.; Tubiana, M.; Lê, M.G.; Valleron, A.J.; Mouriesse, H.; Contesso, G.; Sarrazin, D. Breast cancer: Relationship between the size of the primary tumor and the probability of metastatic dissemination. *Br. J. Cancer* **1984**, *49*, 709–715. [[CrossRef](#)] [[PubMed](#)]
74. Koscielny, S.; Tubiana, M. The link between local recurrence and distant metastases in human breast cancer. *Int. J. Radiat. Oncol. Biol. Phys.* **1999**, *43*, 11–24. [[CrossRef](#)]
75. Tabar, L.; Duffy, S.W.; Vitak, B.; Chen, H.H.; Prevost, T.C. The natural history of breast carcinoma: What have we learned from screening? *Cancer* **1999**, *86*, 449–462. [[CrossRef](#)]
76. Tubiana, M.; Koscielny, S. The natural history of breast cancer and the link between local recurrence and distant metastases: Implications for therapy. *Rep. Pract. Oncol. Radiother.* **2001**, *6*, 181–195. [[CrossRef](#)]
77. Koscielny, S.; Arriagada, R.; Adolfsson, J.; Fornander, T.; Bergh, J. Impact of tumor size on axillary involvement and distant dissemination in breast cancer. *Br. J. Cancer* **2009**, *101*, 902–907. [[CrossRef](#)]
78. Yu, K.D.; Jiang, Y.Z.; Chen, S.; Cao, Z.G.; Wu, J.; Shen, Z.Z.; Shao, Z.M. Effect of large tumor size on cancer-specific mortality in node-negative breast cancer. *Mayo Clin. Proc.* **2012**, *87*, 1171–1180. [[CrossRef](#)]
79. Lin, R.S.; Plevritis, S.K. Comparing the benefits of screening for breast cancer and lung cancer using a novel natural history model. *Cancer Causes Control* **2012**, *23*, 175–185. [[CrossRef](#)]
80. Narod, S.A. Tumor size predicts long-term survival among women with lymph node-positive breast cancer. *Curr. Oncol.* **2012**, *19*, 249–253. [[CrossRef](#)]
81. Narod, S.A.; Iqbal, J.; Jakubowska, A.; Huzarski, T.; Sun, P.; Cybulski, C.; Gronwald, J.; Byrski, T.; Lubinski, J. Are two-centimeter breast cancers large or small? *Curr. Oncol.* **2013**, *20*, 205–211. [[CrossRef](#)]
82. Elkin, E.B.; Hudis, C.; Begg, C.B.; Schrag, D. The effect of changes in tumor size on breast carcinoma survival in the U.S.: 1975–1999. *Cancer* **2005**, *104*, 1149–1157. [[CrossRef](#)] [[PubMed](#)]
83. Tevaarwerk, A.J.; Gray, R.J.; Schneider, B.P.; Smith, M.L.; Wagner, L.I.; Fetting, J.H.; Davidson, N.; Goldstein, L.J.; Miller, K.D.; Sparano, J.A. Survival in patients with metastatic recurrent breast cancer after adjuvant chemotherapy: Little evidence of improvement over the past 30 years. *Cancer* **2013**, *119*, 1140–1148. [[CrossRef](#)] [[PubMed](#)]
84. Jemal, A.; Ward, E.M.; Johnson, C.J.; Cronin, K.A.; Ma, J.; Ryerson, B.; Mariotto, A.; Lake, A.J.; Wilson, R.; Sherman, R.L.; et al. Annual Report to the Nation on the Status of Cancer, 1975–2014, Featuring Survival. *J. Natl. Cancer Inst.* **2017**, *109*, dxx030. [[CrossRef](#)] [[PubMed](#)]

85. Zheng, Y.Z.; Wang, L.; Hu, X.; Shao, Z.M. Effect of tumor size on breast cancer-specific survival stratified by joint hormone receptor status in a SEER population-based study. *Oncotarget* **2015**, *6*, 22985–22995. [[CrossRef](#)]
86. Sopik, V.; Narod, S.A. The relationship between tumor size, nodal status and distant metastases: On the origins of breast cancer. *Breast Cancer Res. Treat.* **2018**, *170*, 647–656. [[CrossRef](#)]
87. Orang, E.; Marzony, E.T.; Afsharfard, A. Predictive role of tumor size in breast cancer with axillary lymph node involvement—Can size of primary tumor be used to omit an unnecessary axillary lymph node dissection? *Asian Pac. J. Cancer Prev.* **2013**, *14*, 717–722. [[CrossRef](#)]
88. Jung, J.; Suh, Y.J.; Ko, B.K.; Lee, E.S.; Kim, E.K.; Paik, N.S.; Byun, K.D.; Hwang, K.T. Clinical implication of subcategorizing T2 category into T2a and T2b in TNM staging of breast cancer. *Cancer Med.* **2018**, *7*, 5514–5524. [[CrossRef](#)]
89. Narod, S.A.; Giannakeas, V.; Sopik, V. Time to death in breast cancer patients as an indicator of treatment response. *Breast Cancer Res. Treat.* **2018**, *172*, 659–669. [[CrossRef](#)]
90. Kirch, R.L.; Klein, M. Prospective evaluation of periodic breast examination programs. *Cancer* **1976**, *38*, 265–272. [[CrossRef](#)]
91. Heuser, L.; Spratt, J.S., Jr.; Polk, H.C., Jr.; Buchanan, J. Relation between mammary cancer growth kinetics and the intervals between screenings. *Cancer* **1979**, *43*, 857–862. [[CrossRef](#)]
92. Heuser, L.; Spratt, J.S.; Polk, H.C., Jr. Growth rates of primary breast cancers. *Cancer* **1979**, *43*, 1888–1894. [[CrossRef](#)]
93. Spratt, J.S.; Heuser, L.; Kuhns, J.G.; Reiman, H.M.; Buchanan, J.B.; Polk, H.C., Jr.; Sandoz, J. Association between the actual doubling times of primary breast cancer with histopathologic characteristics and Wolfe’s parenchymal mammographic patterns. *Cancer* **1981**, *47*, 2265–2268. [[CrossRef](#)]
94. Begg, A.C.; McNally, N.J.; Shrieve, D.C.; Karcher, H. A method to measure the duration of DNA synthesis and the potential doubling time from a single sample. *Cytometry* **1985**, *6*, 620–626. [[CrossRef](#)] [[PubMed](#)]
95. Arnerlöv, C.; Emdin, S.O.; Lundgren, B.; Roos, G.; Söderström, J.; Bjersing, L.; Norberg, C.; Angquist, K.A. Breast carcinoma growth rate described by mammographic doubling time and S-phase fraction. Correlations to clinical and histopathologic factors in a screened population. *Cancer* **1992**, *70*, 1928–1934. [[CrossRef](#)]
96. Arnerlöv, C.; Emdin, S.O.; Lundgren, B.; Roos, G.; Söderström, J.; Bjersing, L.; Norberg, C.; Angquist, K.A. Mammographic growth rate, DNA ploidy, and S-phase fraction analysis in breast carcinoma. A prognostic evaluation in a screened population. *Cancer* **1992**, *70*, 1935–1942. [[CrossRef](#)]
97. Bailey, S.L.; Sigal, B.M.; Plevritis, S.K. A simulation model investigating the impact of tumor volume doubling time and mammographic tumor detectability on screening outcomes in women aged 40–49 years. *J. Natl. Cancer Inst.* **2010**, *102*, 1263–1271. [[CrossRef](#)]
98. Vieira, I.T.; de Senna, V.; Harper, P.R.; Shahani, A.K. Tumor doubling times and the length bias in breast cancer screening programmes. *Health Care Manag. Sci.* **2011**, *14*, 203–211. [[CrossRef](#)]
99. Fornvik, D.; Lang, K.; Andersson, I.; Dustler, M.; Borgquist, S.; Timberg, P. Estimates of breast cancer growth rate from mammograms and its relation to tumor characteristics. *Radiat. Prot. Dosim.* **2016**, *169*, 151–157. [[CrossRef](#)]
100. Seely, J.M.; Alhassan, T. Screening for breast cancer in 2018—what should we be doing today? *Curr. Oncol.* **2018**, *25*, S115–S124. [[CrossRef](#)]
101. Wu, Q.; Li, J.; Zhu, S.; Wu, J.; Chen, C.; Liu, Q.; Wei, W.; Zhang, Y.; Sun, S. Breast cancer subtypes predict the preferential site of distant metastases: A SEER based study. *Oncotarget* **2017**, *8*, 27990–27996. [[CrossRef](#)]
102. Wu, S.G.; Li, H.; Tang, L.Y.; Sun, J.Y.; Zhang, W.W.; Li, F.Y.; Chen, Y.X.; He, Z.Y. The effect of distant metastases sites on survival in de novo stage-IV breast cancer: A SEER database analysis. *Tumor Biol.* **2017**, *39*, 1010428317705082. [[CrossRef](#)] [[PubMed](#)]
103. Wang, H.; Zhang, C.; Zhang, J.; Kong, L.; Zhu, H.; Yu, J. The prognosis analysis of different metastasis pattern in patients with different breast cancer subtypes: A SEER based study. *Oncotarget* **2017**, *8*, 26368–26379. [[CrossRef](#)] [[PubMed](#)]
104. Xiao, W.; Zheng, S.; Yang, A.; Zhang, X.; Zou, Y.; Tang, H.; Xie, X. Breast cancer subtypes and the risk of distant metastasis at initial diagnosis: A population-based study. *Cancer Manag. Res.* **2018**, *10*, 5329–5338. [[CrossRef](#)] [[PubMed](#)]

105. Yao, Y.; Chu, Y.; Xu, B.; Hu, Q.; Song, Q. Risk factors for distant metastasis of patients with primary triple-negative breast cancer. *Biosci. Rep.* **2019**, *39*, BSR20190288. [[CrossRef](#)]
106. Chen, Q.F.; Huang, T.; Shen, L.; Wu, P.; Huang, Z.L.; Li, W. Prognostic factors and survival according to tumor subtype in newly diagnosed breast cancer with liver metastases: A competing risk analysis. *Mol. Clin. Oncol.* **2019**, *11*, 259–269. [[CrossRef](#)]



© 2020 by the authors. Licensee MDPI, Basel, Switzerland. This article is an open access article distributed under the terms and conditions of the Creative Commons Attribution (CC BY) license (<http://creativecommons.org/licenses/by/4.0/>).